Absolute multiple-ionization cross sections of noble gases by He^+

A. C. F. Santos,* W. S. Melo,† M. M. Sant'Anna, G. M. Sigaud, and E. C. Montenegro
Departamento de Física, Pontifícia Universidade Católica do Rio de Janeiro, Caixa Postal 38071, Rio de Janeiro, RJ 22452-970, Brazil
(Received 01 February 2001; published 16 May 2001)

Absolute multiple-ionization cross sections, σ^{q+}, of He ($q=1,2$), Ne ($q=1$, 2, and 3), Ar ($q=1$, 2, and 3), Kr ($q=1$, 2, and 3), and Xe ($q=1$, 2, 3, and 4) atoms have been determined for interactions with He^+ ions in the 1.0–3.5-MeV impact energy range. Special care was taken to obtain the slow recoil-ion detection efficiencies, by measuring the recoil ions in coincidence with the C^{3+} capture channel and comparing these results with absolute single measurements. Comparison is made with the data available in the literature. The present results are in good agreement with the previously published data in the case of the helium target, but some nonsystematic discrepancies appear for heavier targets.

DOI: 10.1103/PhysRevA.63.062717 PACS number(s): 34.50.Fa, 52.20.Hv

I. INTRODUCTION

Multiple ionization of atoms by ions is one of the fundamental processes in atomic physics with important applications in plasma physics, fusion, upper atmosphere studies, and many others technological areas. Due to this broad range of applications and also due to its role in the study of atomic collision dynamics, there have been great efforts, both experimental and theoretical, to improve our understanding of the ionization processes resulting from ion impact with atoms.

The description of multiple ionization is far from a simple task mainly due to the complexity of the many possible pathways leading to it. For example, double ionization of atoms by fast ions is usually understood in terms of three mechanisms [1]: the shake-off process, in which a first electron is ejected in a direct interaction with the projectile, while the second electron is ionized by the final-state rearragement; a two-step process in which both electrons are simultaneously ejected by the direct interaction with the projectile; and the ionization of an inner-shell electron with a postcollisional Auger decay. Both the shake-off and the inner-shell ionization plus Auger decay yield a double-ionization cross section, σ^{2+}, essentially proportional to the single ionization, σ^{+}. The two-step mechanism, which turns out to be dominant in the intermediate-velocity regime, does not follow this pattern because it is based on the action of the projectile over the two active electrons. As a general rule, the dependences of the multiple-ionization cross sections on the projectile energy and charge state are significantly different from those of single-ionization cross sections. The statistical distribution of the various available inelastic alternatives, as well as the way the electrons dynamically correlate, significantly change the dependence of the multiple-ionization cross section on the projectile energy and the charge state with respect to the single ionization, and need to be considered in detail to understand the multiple ionization.

A widely-used approach for interpretation of the multiple-ionization process is the independent-particle model (IPM), where it is assumed that the ionization of one electron is independent of the others and the related probabilities are given by the binomial distribution [2–5]. This method depends strongly on the quality of the calculations of the single-electron ionization probabilities [5,6] although some general quantitative estimates can be obtained through a simple semiclassical calculation using hydrogenic wave functions [3,4].

An alternative aproach to the IPM is the statistical energy-deposition model, which has also been used by several authors [7–10]. It was formulated by Russek and Thomas [8] and further developed by Cocke [9] and Kabachnick *et al.* [10]. It is based on the hypothesis that the probability for multiple ionization is directly related to the energy deposited by the projectile on the target, which is, in a second step, statistically distributed among all atomic electrons, one or more of which eventually autoionize to the final state.

One parameter to which these calculations are quite sensitive, mainly in the intermediate-velocity regime, is the projectile charge state. The simplest case, i.e., single ionization of light atoms and molecules by structureless charged particles, at high impact velocities, is well described within the framework of the Bethe theory [11]. Deviations of the charge-state scaling from the first Born approximation are expected to be observed either if the collision regime is nonperturbative or if multiple-ionization occurs. These cases were investigated mostly for highly stripped ions [12–14], where the projectile charge state is essentially independent of the impact parameter. If the projectile charge state is small, its influence is more subtle because the screening associated with the projectile can be strongly dependent on the impact parameter. A limiting case where the influence of the screening can be large occurs in stripping collisions with neutral atoms, where the full screening of the target nucleus makes the projectile ionization strongly dependent on the impact parameter [15–19]. These studies, however, concentrated on the single ionization of few-electron ions and studies on the effect of partial screening on multiple-ionization are pratically nonexistent. To the authors knowledge, there are no

*Present address: Instituto de Química, Universidade Federal do Rio de Janeiro, Cidade Universitária, RJ, Brazil.

†Present address: CNRS, Laboratoire Aimé Cotton, 91405 Orsay Cedex, France.

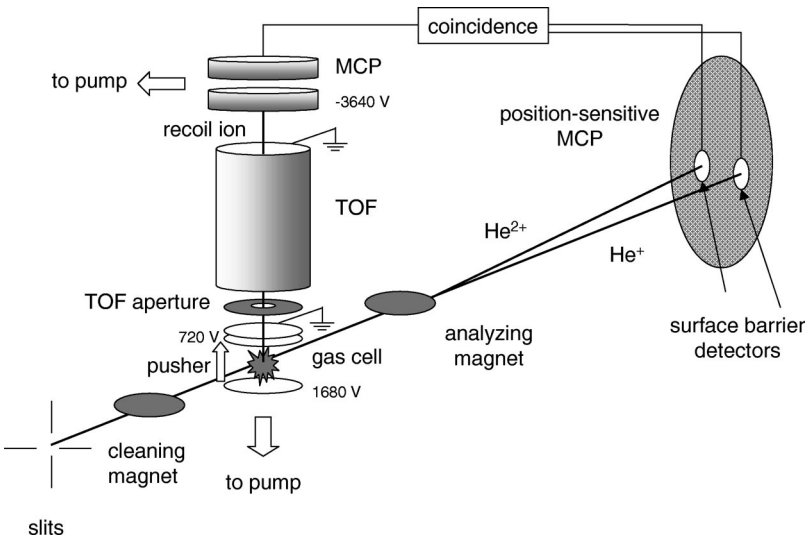

FIG. 1. Schematic diagram of the apparatus used in the present measurements. For details see text.

reliable calculations available for partial multiple ionization of the whole set of noble gases by dressed, low-charge-state projectiles such as He^+, although this charge state is the one that energetic α particles have to go through as they penetrate in matter, a scenario which appears in several applications.

The experimental support for guidance towards further theoretical improvements is presently not satisfactory. Absolute partial multiple-ionization cross sections are scarce and several measurements on multiple target ionization do not determine the final charge state of the recoiling ion, i.e., reporting only total electron and ion production cross sections. For example, in the case of He^+ projectiles, the only data available for partial multiple-ionization of noble gases, overlapping the energy range investigated in this paper, is from DuBois [20].

In this work, we have carried out absolute measurements of partial, multiple-ionization cross sections of He^+ projectiles on He, Ne, Ar, Kr, and Xe, using coincidence techniques, in the energy range from 1.0 to 3.5 MeV. In Sec. II the experiment is described in detail, in Sec. III the results are presented and compared with some calculations and with previous measurements, and in Sec. IV some concluding remarks are made. Except where otherwise stated, the cross sections σ^{q+} noted without subscripts are for ionizing collisions where the projectiles retain their charge state after the interaction. The superscript indicates the charge state of the target after the interaction.

II. EXPERIMENT

A collimated, monoenergetic He^+ ion beam is delivered by the 4-MV Van de Graaff accelerator of the Catholic University of Rio de Janeiro. Figure 1 shows schematically the experimental apparatus, not to scale. Before entering a windowless gas cell, the beam is charge-analyzed by a magnet placed just at the entrance of the gas cell in order to separate the main beam from spurious ones. The two measured emergent charge states, He^+ and He^{2+}, are charge-analyzed by a second magnet and recorded by two surface barrier detectors housed in a detection chamber placed 4 m downstream of the gas cell. The multiply ionized recoil ions produced by the primary beam, under single collision conditions, are accelerated by a two-stage electric field and detected by two microchannel plate detectors in a chevron configuration. They provide the stop signal to two time-to-amplitude converters started by the signals from the surface barrier detectors. The first stage of the electric field (pusher) consists of a plate-grid system [21] with the primary beam passing through its middle and with a 960-V/cm electric field. The second stage is a lens, with a 3600-V/cm electric field, designed to make a weak focusing of the recoil ions in a 4-mm diameter aperture placed 3.7 cm from the interaction region (''TOF aperture'' in Fig. 1). The accelerating potentials were chosen with the aid of the SIMION program [22] and the simulation gives a negligible dependence of the recoil-ion trajectories on the charge-to-mass ratio. The gas cell has an effective length of 72 mm [23].

The gas cell has a cylindrical shape with 11-cm diameter and 15-cm height. Its volume, approximately 1.4 l, is large enough to assure that the pressure measurement inside the cell, made by an absolute capacitive manometer (MKS-Baratron), is not affected by the leak through the appertures [21]. The aperture on the time-of-flight tube, together with two others with diameters of 1.8 and 2.0 mm placed at the beam entrance and exit of the gas cell, respectively, assures a differential pressure ratio of 1:300 between the outer chamber and the gas cell. We observed that the absolute detection efficiency of the microchannel plate detector (MCP) depends both on the pressure and on the gas composition around the MCP. The atoms or molecules in the electron path can be ionized giving rise to additional electrons and increasing the detection efficiency. In order to avoid this effect, the region housing the MCP is pumped by a 200-l s^{-1} diffusion pump located underneath the MCP so that the pressure in its vicinity does not change when the pressure or the gas type is changed in the gas cell. This procedure ensures that the recoil-ion detection system is independent of the loading conditions of the gas cell. Figure 2 shows the time-of-flight spectrum, expressed in terms of mass over charge ratio, for

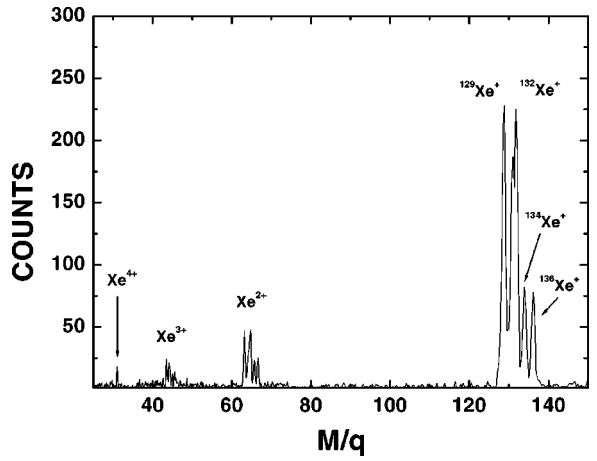

FIG. 2. Time-of-flight mass spectrum of Xe corresponding to the ionization by 2.0 MeV He^+.

the ionization channel of 2.0-MeV He^+ ions on Xe. This figure gives an illustration of the time resolution of our coincidence circuitry, showing a clear separation of the isotopic components of the Xe ions, as well as the low background present in the measurements.

In the detection chamber placed at the end of the beamline, an *x-y* position-sensitive microchannel plate detector was used to locate spurious beams originating from charge-changing collisions of the main beam with the residual gas inside the beamline before the gas cell (Fig. 1). The spurious beams were carefully identified before the proper positioning of the surface barrier detectors. The counting rates of incident projectiles on the surface barrier detectors were kept below $1.5\times10^3\ s^{-1}$ in order to prevent signal deterioration.

The cross sections were obtained by keeping the pressure inside the gas cell at 1.0 mTorr for the He, Ne, and Ar, 0.8 mTorr for Kr, and 0.5 mTorr for the Xe targets to ensure single-collision conditions and a correct operation of the microchannel plate detector. The growth-rate method was used to determine the single-ionization yields, as well as the ratio of multiple-to-single yields. This last quantity was found to be constant in a range of pressures including those specified above.

Special care was taken to obtain the detection efficiencies of the multiply charged recoil ions. This was achieved by measuring the recoil ions in coincidence with the single capture of C^{3+} on noble gases [24] and comparing these measurements with the single measurements for this channel (see below). It is well known that the efficiency of the microchannel plate detector is a function of the impact energy of the ionic species. The absolute detector efficiency increases with the ion energy and reaches a saturation for impact energies greater than 3 KeV [25,26]. We observed that for negative polarization potentials above 3300 V, the detection efficiency is independent of the impacting particle. To guarantee being in the saturation region, the front plate of the microchannel plate detector was polarized with -3640 V.

The integrated coincidence signal I^{q+}, subtracted from a linear background, where q is the final charge state of the target, is proportional to the beam intensity I_0, the number of target scattering centers per volume $n(P)$, where P is the target pressure, the effective target length l_{eff}, the cross section σ^{q+}, and the recoil ion detection efficiency ϵ^{q+}. The efficiency of the surface barrier detector was assumed to be unity. Thus, we have

$$I^{q+}=\epsilon^{q+}l_{eff}I_0n(P)\sigma^{q+}. \tag{1}$$

In order to measure the recoil-ion detection efficiencies ϵ^{q+}, we carried out simultaneous single and coincidence measurements of single electron-capture cross sections of C^{3+} on helium, neon, argon, krypton, and xenon, with projectile energies between 1.3 and 3.5 MeV. In the following, the electron-capture cross section producing a recoil ion with charge q is denoted by σ_{32}^{q+}, while the total electron capture cross section is denoted by σ_{32}. The σ_{32} cross section is absolutely determined by measuring the fraction of the main beam that performs charge-changing collisions [19], and σ_{32}^{q+} is determined by measuring the target multiply charged recoil ions in coincidence with the C^{2+} emergent beam. These cross sections are related by

$$\sigma_{32}=\sum_q \sigma_{32}^{q+}, \tag{2}$$

or, using Eq. (1),

$$\sigma_{32}=\sum_q \frac{I^{q+}}{\epsilon^{q+}l_{eff}I_on(P)}. \tag{3}$$

As a first step to determine ϵ^{q+}, we measured the ratios of multiple-to-single ionization cross sections $(\sigma^{q+}/\sigma^{1+})$ for different projectiles, different projectile energies, and various targets, and compared these measurements with results found in the literature, such as multiple-ionization by protons [27], C^{3+} [28], and He^+ [20]. From Eq. (1), these ratios can be written as

$$\frac{\sigma^{q+}}{\sigma^{1+}}=\frac{\epsilon^{+}I^{q+}}{\epsilon^{q+}I^{+}}. \tag{4}$$

The set of ratios $\epsilon^{q+}/\epsilon^{+}$ were found to be close to unity for all charge states and collision systems studied within 30% of uncertainty. This indicates that the detection efficiency, in our recoil-ion detection system, can be considered essentially independent of the recoil-ion charge state, so that we can make $\epsilon^{q+}\simeq\epsilon$, take them out of the summation in Eq. (2), and rewrite this equation as

$$\epsilon=\frac{1}{\sigma_{32}}\sum_q \frac{I^{q+}}{l_{eff}I_on(P)}. \tag{5}$$

Using Eq. (5) for C^{3+} projectiles with various energies impinging on different targets, we found for ϵ a value independent of the target atomic number. The absolute cross section is obtained by substituting ϵ^{q+} for this value of ϵ in Eq. (1).

The measurements of the relative intensities for different charge states are sensitive to variations in the electronic dis-

TABLE I. Single- and double-ionization cross sections of He by He^+ (Mb).

E (MeV)	He^+	He^{2+}
1.00	88±13	2.9±0.6
1.25	70±10	1.9±0.4
1.50	66±10	1.3±0.3
2.00	56±8	1.1±0.2
2.50	45±6	0.73±0.15
3.00	38±6	0.45±0.09
3.50	33±5	0.27±0.05

TABLE III. Single-, double-, and triple-ionization cross sections of Ar by He^+ (Mb).

E (MeV)	Ar^+	Ar^{2+}	Ar^{3+}
1.00	229±34	30±5	6.1±1.2
1.50	206±31	21±4	2.3±0.5
2.00	162±24	17±3	2.4±0.5
2.50	132±20	11±2	1.7±0.3
3.00	134±20	8.5±1.4	1.5±0.3
3.50	108±16	9.1±1.5	1.3±0.3

crimination threshold settings, to the background gas pressure, and, as mentioned before, to the ion impact velocity on the detector. For instance, the threshold effect arises because all recoil ions are accelerated through the same potential field. In this way, multiply charged ions hit the detector at higher energies than the singly charged species, giving rise to pulse-height distributions with maxima shifted to higher pulse heights. Counts from the single charged pulse-height distribution can be lost at a faster rate than those from multiply charged distributions if the discrimination threshold is increased. In addition, the recoil ion can perform charge transfer collisions with background gas molecules in the time-of-flight tube. Special care was taken to keep these sources of uncertainties minimized.

The main sources of uncertainties in the coincidence measurements come from impurities in the gas targets due to the gas-admittance system ($\sim$1–3%), the determination of the product of the detection efficiency by the effective length of the gas cell ($\sim$10%), counting statistics, and random coincidence subtraction (up to $\sim$15%). The overall uncertainties range between 15 and 30%.

In the present experiment, some measured ionic charge states cannot be separated by their flight times from background impurity ions because they have the same mass-to-charge ratio (H_2^+ from He^{2+}; N_2^+ and CO^+ from Kr^{3+}; N^+, N_2^{+2}, and O_2^{2+} from Kr^{6+} and Ar^{3+}). These contaminations are estimated to be smaller than 3%.

III. RESULTS AND DISCUSSION

The results from our measurements for multiple-ionization of He, Ne, Ar, Kr, and Xe by He^+ projectiles are listed in Tables I–V, respectively. In Fig. 3 we present our results compared with the available experimental data for He^+ projectiles as well as with single ionization by protons taken from Ref. [27]. Comparison with protons will be restricted to the single-ionization cross sections, where distant collisions play a major role and He^+ can be approximately considered as a structureless projectile with charge equal to unity. In the following, we present a detailed discussion only for the He and Ne cases, because the heavier gases present the same general features as Ne. Overall, our results for all final charge states of the target present good agreement with the previous data, where overlapping measurements from other authors occur. In all cases we restrict our analysis to the intermediate-to-high velocity regime, where our measurements were carried out.

The present measurements for single and double ionization of He by He^+ are compared with the results of DuBois [20] and Forest *et al.* [29]. The single ionization by protons from DuBois *et al.* [27] is also shown. Our results are in a very good agreement with the previously published data for He^+ projectiles over the entire energy range investigated.

The comparison of He^+ with single-ionization cross sections by protons is carried out to show differences emerging when dressed or bare projectiles are used in the ionization process. For protons, the projectile charge is the same for all impact parameters, while in the He^+ case the projectile charge increases if the impact parameter decreases. Thus, for each energy, dressed projectiles should have effective charges that range between the ion charge and the nuclear charge, giving, in principle, a total ionization cross section that is larger when compared with the proton case. However, if the collision is close enough, there is also a possibility of the projectile electron being stripped along the ionizing collision. Because our measurements are constrained to the cases where He^+ also appears in the exit channel, this re-

TABLE II. Single-, double-, and triple-ionization cross sections of Ne by He^+ (Mb).

E (MeV)	Ne^+	Ne^{2+}	Ne^{3+}
1.00	116±17	15±2	2.4±0.6
1.50	76±11	8.3±1.3	0.86±0.22
2.00	82±12	7.5±1.2	0.80±0.20
2.50	64±10	5.3±0.8	0.50±0.13
3.00	69±10	4.9±0.8	
3.50	66±10	4.4±0.7	

TABLE IV. Single-, double-, and triple-ionization cross sections of Kr by He^+ (Mb).

E (MeV)	Kr^+	Kr^{2+}	Kr^{3+}
1.00	262±39	47±8	14±2
1.50	179±27	23±4	9.1±1.6
2.00	159±24	23±4	9.2±1.7
2.50	137±21	18±3	9.4±1.7
3.00	133±20	14±2	5.8±1.0
3.50	123±18	12±2	4.7±0.8

TABLE V. Single-, double-, triple-, and quadruple-ionization cross sections of Xe by He^+ (Mb).

E (MeV)	Xe^+	Xe^{2+}	Xe^{3+}	Xe^{4+}
1.00	290±44	41±7	16±3	10±2
1.50	219±33	32±5	14±3	6.1±1.3
2.00	175±26	27±5	11±2	5.0±1.0
2.50	168±25	27±5	10±2	4.9±1.0
3.00	146±22	24±4	10±2	4.3±0.9
3.50	132±20	20±3	8.2±1.6	4.7±1.0

striction imposes a decrease of the ionization probability, as compared with bare projectiles, for close collisions. This last effect counterbalances the increase of the ionization probability due to the increase of the screened nuclear charge for close collisions and the net result depends both on the projectile energy and target atomic number. For the He target case, the proton data are clearly below our He^+ data. Indeed, as the perturbing effect of the He target over the projectile electron is not too high, the increase of the He^+ effective charge in close collisions results effectively in an increase of the ionization cross section as compared with the proton case.

The present data for single ionization of Ne are 25–40 % smaller than those of DuBois [20] for the energies where overlap between the two measurements occurs. Those are the only data available in the literature. In the case of double ionization, the results of DuBois are about 50% higher, and for the triple-ionization channel, the difference between the two sets of data reaches 80% at 2.0 MeV. Although the time-of-flight spectrometer resolution was good enough to completely separate ^{20}Ne from its isotope ^{22}Ne, the data shown in Table II represent the sum of both isotopes. The mean recoil-ion charge state ($\Sigma q\sigma^{q+}/\Sigma\sigma^{q+}$) is 1.14 at 1 MeV and is weakly dependent on the projectile energy.

In contrast with the He case, the comparison between the Ne single-ionization cross section by protons and He^+ shows a clear superposition of the data in the high-energy region, with a slight tendency of the latter to be below the former, behavior that can also be observed for the other gases heavier than Ne. These close values obtained for the cross sections by these two projectiles are also given by the theoretical calculations of Kirchner *et al.* [5,6], based on the independent-particle model and considering transitions involving all active electrons, both from the projectile and the target. The restriction imposed by the measurements in which the ionization is carried out without electron loss makes the contribution from collisions with small impact parameters to be very small. Indeed, the strength of the perturbing field of the heavy target over the projectile increases sharply towards a high value for decreasing internuclear distances near the atomic radius. This strong field saturates the electron-loss probability, which becomes nearly equal to unity for impact parameters smaller than the atomic radius [16,18]. Thus, only distant collisions are allowed if there is no electron loss, causing the effective charge of the projectile for such allowed collisions to be near one. This effect becomes more evident as the target atomic number increases.

The calculations by Kirchner [6] for double and triple ionization of Ne show the same high-energy trend presented by the experiments, although the absolute values for the cross sections are higher than our measurements. For protons, the ionization of the *K*-shell electrons with a subsequent Auger decay can give some contribution for double and triple ionization at higher energies [5]. This is, however, a branch essentially fed by close collisions which, as mentioned above, are very efficient in stripping the projectile.

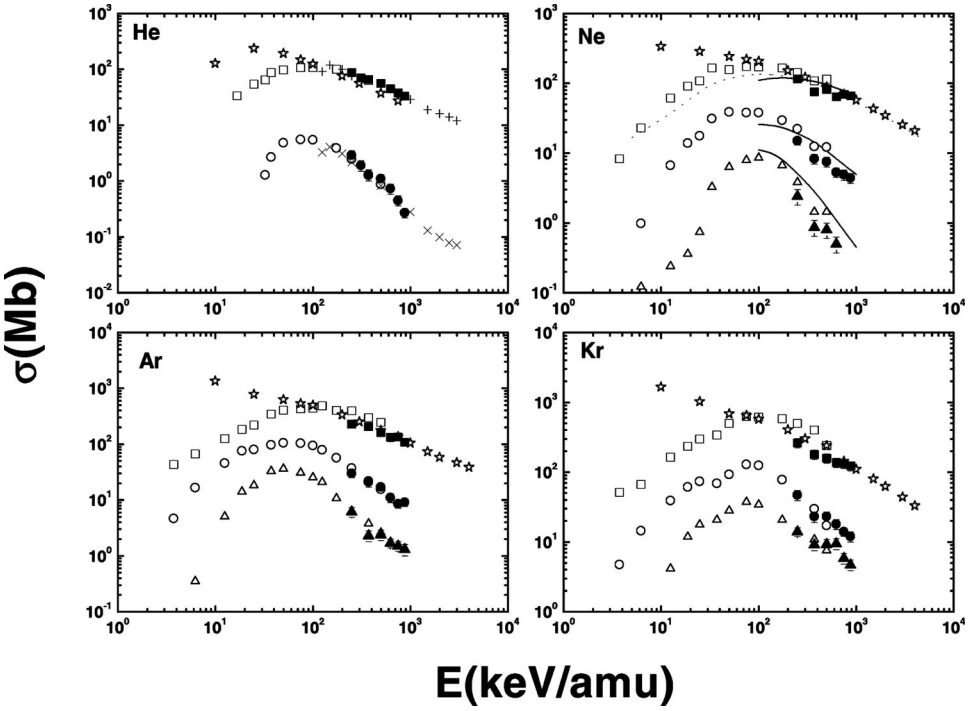

FIG. 3. Single- and double-ionization cross sections of He, single-, double-, and triple-ionization cross sections of Ne, Ar, and Kr by He^+, and single ionization by protons as a function of the projectile energy. He^+ single ionization: closed squares, this work; open squares, Ref. [20]; crosses (+), Ref. [29]. He^+ double ionization: closed circles, this work; open circles, Ref. [20]; crosses (x), Ref. [29]. He^+ triple ionization: closed triangles, this work; open triangles, Ref. [20]. Proton single ionization: open stars Ref. [27]. Full lines: quantum-mechanical calculations for Ne single, double and triple ionization by He^+, Ref. [6]. Dashed line: quantum-mechanical calculations for Ne single ionization by protons, Ref. [5].

Because of that, the contribution from this mechanism to double and triple ionization of Ne by He^+ should be small.

Single-, double-, and triple-direct-ionization cross sections of Ar by He^+ impact are listed in Table III and also shown in Fig. 3, together with the data from DuBois [20]. In the case of single ionization, the present data are about 50% smaller than the results of DuBois [20]. On the other hand, good agreement is found in the cases of double and triple ionization. As in the Ne case, the cross sections for single ionization by protons and by He^+ tend to coalesce at higher energies.

The partial multiple-ionization cross sections for Kr are presented in Table IV and plotted in Fig. 3. For the single ionization, the values from DuBois [20] are higher than the present ones. As in the Ar case, for double and triple ionization there is a good overall agreement between the two sets of data.

In Table V single-, double-, triple-, and quadruple-direct-ionization cross sections of Xe in collisions with He^+ projectiles are presented. To the authors' knowledge, there are no other measurements available in the literature to compare with. As for the previous gases, the partial multiple-ionization cross sections of xenon ($q=1$ up to 4) decrease smoothly with the incident projectile energy. The mean recoil-ion charge state is 1.3 in the energy range studied in this work and the single ionization contributes 65% to the total ion production coming from the direct ionization channel.

A few remarks on previous normalization procedures are pertinent. The cross sections presented by DuBois [20] were normalized to the total absolute positive-ion production reported by Rudd *et al.* [30]. However, the total electron production cross sections presented by DuBois [20] present a deviation from the values of Rudd *et al.* [30]. In an earlier paper [27], DuBois reported cross sections for impact energies smaller than 100 keV normalized to single electron-capture cross sections. Those cross sections resulted in a total ion production 10–15 % smaller than the values published by Rudd *et al.* [30]. The measurements were repeated in order to investigate this discrepancy. The system was independently calibrated without normalization either to single electron capture or to ion production cross sections. The later measurements confirmed the earlier results and the inconsistency between total electron-production cross sections remained. There is no clear reason for the origin of such discrepancies, but it seems from the analysis of the available data, including the present ones, that the total ion production obtained by coincidence measurements apparently presents some discrepancies when compared with noncoincident, charge-collection measurements.

IV. SUMMARY AND CONCLUSIONS

Cross sections for single and multiple-ionization of noble gases by He^+ impact have been measured in the 1.0–3.5-MeV energy range. The detection efficiencies of the slow recoil ions were obtained through a careful measurement of the recoil ions in coincidence with the C^{3+} capture channel in collisions with rare gases and by comparing these results with absolute single measurements. The absolute values of the present set of data are independent of any previous measurements, thus providing an independent reference for studies of multielectronic processes in the intermediate-to-high velocity regime.

Theoretical studies of multiple-ionization by dressed projectiles are almost inexistent and we compared our Ne results with recent quantum mechanical calculations by Kirchner *et al.* [5,6]. The comparison shows increasing discrepancies between theory and experiment as the recoil-ion charge states increase, but a more conclusive analysis of the reasons for this behavior can be achieved only by considering the other gases. It is also clear from the analysis presented above that electron loss has a major influence in the *n*-fold target ionization as the former process strongly affects close collisions, inhibiting them from contributing to ionization. This is also true for the inner-shell ionization plus Auger decay contribution for multiple-ionization because of the predominance of close collisions in inner-shell ionization. The comparison between bare and dressed projectiles with similar charge is thus a powerful methodological approach towards the understanding of the dynamics, which is behind close and distant collisions in multielectron ionization.

ACKNOWLEDGMENTS

We thank Robert D. DuBois for the many and elucidating discussions about experiments of this kind. This work was supported in part by the Brazilian agencies CNPq, FINEP, CAPES, FAPERJ, MCT (PRONEX), and by the Volkswagen-Stiftung (Germany).

[1] J.H. McGuire, Phys. Rev. Lett. **49**, 1153 (1982).
[2] J.H. McGuire, Adv. At., Mol., Opt. Phys. **29**, 217 (1992).
[3] A.B. Voitkiv and A.V. Koval, J. Phys. B **29**, 2661 (1996).
[4] M.M. Sant'Anna, E.C. Montenegro, and J.H. McGuire, Phys. Rev. A **58**, 2148 (1998).
[5] T. Kirchner, H.J. Lüdde, and R.M. Dreizler, Phys. Rev. A **61**, 012705 (1999).
[6] T. Kirchner (private communication); T. Kirchner and M. Horbatsch, Phys. Rev. A **63**, 062718 (2001).
[7] J.H. McGuire, N. Stolterfoht, and P.R. Simony, Phys. Rev. A **24**, 97 (1981).
[8] A. Russek and M.T. Thomas, Phys. Rev. A **109**, 2015 (1958).
[9] C.L. Cocke, Phys. Rev. A **20**, 749 (1979).
[10] N.M. Kabachnik, V.N. Kondratyev, Z. Roller-Lutz, and H.O. Lutz, Phys. Rev. A **56**, 2848 (1997).
[11] M. Inokuti, Rev. Mod. Phys. **43**, 297 (1971).
[12] A.S. Schlachter, K.H. Berkner, W.G. Graham, R.V. Pyle, P.J. Schneider, K.R. Stalder, J.W. Sterns, J.A. Tanis, and R.E. Olson, Phys. Rev. A **23**, 2331 (1981).
[13] H.K. Haugen, L.H. Andersen, P. Hvelplund, and H. Knudsen, Phys. Rev. A **26**, 1962 (1982).
[14] T. Matsuo, T. Kohno, S. Makino, M. Mizutani, T. Tonuma, A.

Kitagawa, T. Murakami, and H. Tawara, Phys. Rev. A **60**, 3000 (1999).
[15] E.C. Montenegro, W.E. Meyerhof, and J.H. McGuire, Adv. At., Mol., Opt. Phys. **34**, 249 (1994).
[16] M.M. Sant'Anna, W.S. Melo, A.C.F. Santos, G.M. Sigaud, and E.C. Montenegro, Nucl. Instrum. Methods Phys. Res. B **99**, 46 (1995).
[17] E.C. Montenegro, K.L. Wong, W. Wu, P. Richard, I. Ben-Itzhak, C.L. Cocke, R. Moshammer, J.P. Giese, Y.D. Wang, and C.D. Lin, Phys. Rev. A **55**, 2009 (1997).
[18] A.E. Voitkiv, G.M. Sigaud, and E.C. Montenegro, Phys. Rev. A **59**, 2794 (1999).
[19] W.S. Melo, M.M. Sant'Anna, A.C.F. Santos, G.M. Sigaud, and E.C. Montenegro, Phys. Rev. A **60**, 1124 (1999).
[20] R.D. DuBois, Phys. Rev. A **39**, 4440 (1989).
[21] E.C. Montenegro, W.S. Melo, W.E. Meyerhof, and A.G. Pinho, Phys. Rev. A **48**, 4259 (1993).
[22] D. A. Dahl, The SIMION 3D version 6.0 User's Manual (Idaho National Engineering Laboratory, 1995).
[23] H. Tawara and A. Russek, Rev. Mod. Phys. **45**, 2 (1973).
[24] A. C. F. Santos, W. S. Melo, M. M. Sant'Anna, G. M. Sigaud, and E. C. Montenegro (unpublished).
[25] V. Tarnovsky and K. Becker, Z. Phys. D: At., Mol. Clusters **22**, 603 (1992).
[26] M.R. Bruce and R.A. Bonham, Z. Phys. D: At., Mol. Clusters **24**, 149 (1992).
[27] R.D. DuBois, L.H. Toburen, and M.E. Rudd, Phys. Rev. A **29**, 70 (1984); R.D. DuBois, Phys. Rev. Lett. **52**, 2348 (1984).
[28] M. Saito, Y. Haruyama, N. Hamamoto, K. Yoshida, A. Itoh, and N. Imanishi, J. Phys. B **28**, 5117 (1995).
[29] J.L. Forest, J.A. Tanis, S.M. Ferguson, R.R. Haar, and K. Lifrieri, Phys. Rev. A **52**, 350 (1995).
[30] M.E. Rudd, T.V. Goffe, A. Itoh, and R.D. DuBois, Phys. Rev. A **32**, 2 (1985).